

# Phage-antibiotic therapy under density dependent bacterial defenses

Rohan Shirur\* and Bryce Morsky†

Department of Mathematics, Florida State University, Tallahassee, FL,  
USA

December 23, 2025

## Abstract

Phage therapy is an alternative treatment method for bacterial infections. It has shown particular promise in reducing bacterial load while preventing antibiotic resistance. Here, we develop a mathematical model of a bacterial infection within a host to study phage therapy. It incorporates interactions between phages, bacteria, the immune system, and antibiotics. Additionally, the model includes bacterial social dynamics that provide protection from treatments and the innate immune response. We analytically and numerically identify all of the equilibria of the model and derive insights regarding the overall effectiveness of phage therapy. Without phage therapy, the model exhibits bistability: bacteria populations above a threshold grow and become entrenched, while those below it can be effectively suppressed by the immune system. We find that that phages destabilize the former equilibrium, and thus in combination with the immune system are able to suppress the bacteria. We conducted bifurcation analyses, which show that the equilibrium with a suppressed population of bacteria can become unstable. In this scenario, the system undergoes oscillations. However, these oscillations — which can be exacerbated by social dynamics — lead to minuscule bacterial populations, and thus, in practice, phage therapy is widely effective across the parameter space. We also demonstrate how suppression can be further improved by the addition of periodic dosing of antibiotics in a combination therapy.

**Keywords:** antibiotic resistance, combination therapy, immune response, phage therapy, social dynamics

---

\*rs23bs@fsu.edu

†bmorsky@fsu.edu

# 1 Introduction

The healthcare system relies heavily upon antibiotics to combat bacterial infection. However, the overreliance on and misuse of antibiotics have resulted in the emergence of antibiotic resistant strains of bacteria (Barbosa and Levy, 2000) with a continuing evolution of novel antibiotic resistant strains over time (Normark and Normark, 2002). In addition to mutation, antibiotic resistance can be spread rapidly across various bacterial organisms and even different bacterial species by means of horizontal gene transfer (Burmeister, 2015). Thus, alternative treatment options are paramount to sustainably fight bacterial infections. One such treatment is phage therapy, which utilizes bacteriophages, also known as phages, to selectively eliminate bacterial pathogens (Fujiki and Schnabl, 2023; Gordillo Altamirano and Barr, 2019). It has shown significant promise in fighting bacterial infections while minimizing antibiotic resistance. This is due in part to the inherent strain specificity of phages which limits indiscriminate bacterial killing (Zalewska et al., 2025). Trials have even indicated that, unlike antibiotics, phages can leave the gut microbiome (a vital component of the immune system) largely intact when fighting bacterial infection (Fujiki and Schnabl, 2023). Phage therapy has been demonstrated to effectively reduce bacterial load while being well-tolerated by the host with limited side effects (Uyttebroek et al., 2022). It has also achieved therapeutic success at sub-inhibitory concentrations of antibiotics (Rodriguez-Gonzalez et al., 2020). Phage therapy can be implemented along with antibiotics in combination and adaptive therapies, the latter of which incorporate a dynamic treatment approach that adjusts relative to bacterial evolution (Levin and Bull, 2004). Such therapies are primarily done by carefully selecting appropriate phages and drugs, as well as their respective doses, in an attempt to eliminate the pathogenic bacteria within the host while minimizing the proliferation of antibiotic resistance.

Although such therapies are crucial in controlling infection, they are typically complementary to the host's innate immune system, which is the primary mechanism by which bacterial infection is contained and suppressed. The immune response consists of a multifaceted response to neutralize the invading bacteria that adapts and scales based upon the type as well as the quantity of bacteria present (Giamarellos-Bourboulis and Raftogiannis, 2012). The immune system's initial defense mechanism is to deploy white blood cells, specifically neutrophils and macrophages. In the event of a more prolonged infection where the pathogenic bacteria is not immediately suppressed, two other types of white blood cells, T cells and B cells, are deployed by the immune system (Shepherd and McLaren, 2020). T cells kill infected cells and activate other immune responses that can provide long term immunity (Blanden, 1974). Long term immunity is provided by the production of memory T cells, which are able to efficiently identify and respond to previously encountered pathogens (Blanden, 1974). In conjunction with T cells, the innate immune response also deploys B cells, which function to produce antibodies and establish long term adaptive immunity (Akkaya et al., 2020). These B cells are activated around the same time as T cells during the immune response and often require T-helper cell signaling (Akkaya et al., 2020). The primary goal of the immune system when fighting bacterial infection is to not just eradicate harmful bacteria but to instead foster long-term immunity processes that will ensure that the body will be able to adapt and respond to future infections.

In addition to the effects from treatments and the immune system, the overall outcome of a bacterial infection is linked to the behavior of the pathogenic bacteria (Javaudin et al., 2021). Bacteria are social creatures, engaging in cooperative behaviors to coordinate actions to enhance their fitness, increase their chances of survival, and compete for limited resources (West et al., 2007). They exhibit a wide array of social behaviors including, but not limited to, communication, cooperation, and group motility. These cooperative behaviors can result in rapid bacterial growth, increased virulence, and an overall higher bacteria survival rate (Harrison et al., 2006). Bacterial interactions are facilitated by close proximity of bacteria (Ibberson and Whiteley, 2020). Bacteria use a communication method known as quorum sensing to transmit information to one another through the use of autoinducers and thus interact socially (Abisado et al., 2018; Zhao et al., 2018). Quorum sensing can promote biofilm formation, which can prolong their survival and undermine immune responses (Gestel et al., 2015; Kostakioti et al., 2013). Within biofilms, bacteria use chemical and mechanical signals to establish division of labor, resource sharing, and resistance to external threats. These processes can protect bacteria within a host from harmful conditions (Jefferson, 2004). For instance, bacteria within biofilms can benefit from a 100 to 1000 fold increase in antibiotic resistance relative to the resistance of free swimming bacteria (Jarrett et al., 2015). Although these social interactions tend to benefit bacteria, they can also harm them. Current literature suggests that there exists a “goldilocks” zone for bacteria within a system in which they experience maximal social benefit from one another (Ross-Gillespie et al., 2009). At bacterial populations below the optimal range, there are simply not enough bacteria for the colony to truly reap the benefits from social behaviors (West et al., 2007). Bacteria at populations above the optimal range experience significantly more competition for resources, and social interactions at this population level are counterproductive to each cell’s best interests.

In order to effectively understand bacterial infection, phage and combination therapies, and the evolution of antibiotic resistance, it is important that we observe the mechanisms behind the interactions between therapies, the innate immune responses of various hosts, and the behavioral tendencies of bacteria. This process can be observed and analyzed through mathematical modeling techniques. This approach has shown that phage therapy, accounting for the synergistic relationship between phages and the innate immune response, can be effective in protecting normal mice from bacterial infection, but ineffective in neutropenic mice (Leung and Weitz, 2017). It has also demonstrated that the variability in the outcomes of bacterial infection are most closely tied to variability in the bacterial growth rate, strength of the innate immune response, and the activation rate of the immune response (Barber et al., 2021). These systems can be bistable in that infections can lead to the complete elimination of the pathogenic bacteria by the immune system or uncontrolled bacterial growth. In such scenarios, the timing of the immune response is the primary factor determining outcomes, since the treatment works by “buying more time” for the immune system to eradicate the infection and prevent uncontrolled bacterial growth (Flores-Garza et al., 2022).

Bacterial social dynamics, particularly the formation of biofilms and quorum sensing, are a critical component of the outcomes of phage therapy. Biofilms can provide protection from phages (Hansen et al., 2019; Singh et al., 2022). For example, diffusion of phages into and within the biofilm can be hindered by extracellular polymeric substances. Fur-

thermore, phage resistant bacteria can protect phage sensitive bacteria (Simmons et al., 2020), and adsorption can be ineffective due to the close proximity of bacteria (Eriksen et al., 2018). Bacteria can also be protected by employing quorum sensing to reduce phage receptors (Høyland-Kroghsbo et al., 2017). In order to understand the impacts of these defensive capabilities on the success of phage therapy, we developed and analyze a mathematical model that integrates the dynamics between phages, bacteria, antibiotics, and the innate immune response. Our primary focus is on exploring the dynamics of phage therapy and antibiotics in supplementing the innate immune response in fighting bacterial infections.

## 2 Methods

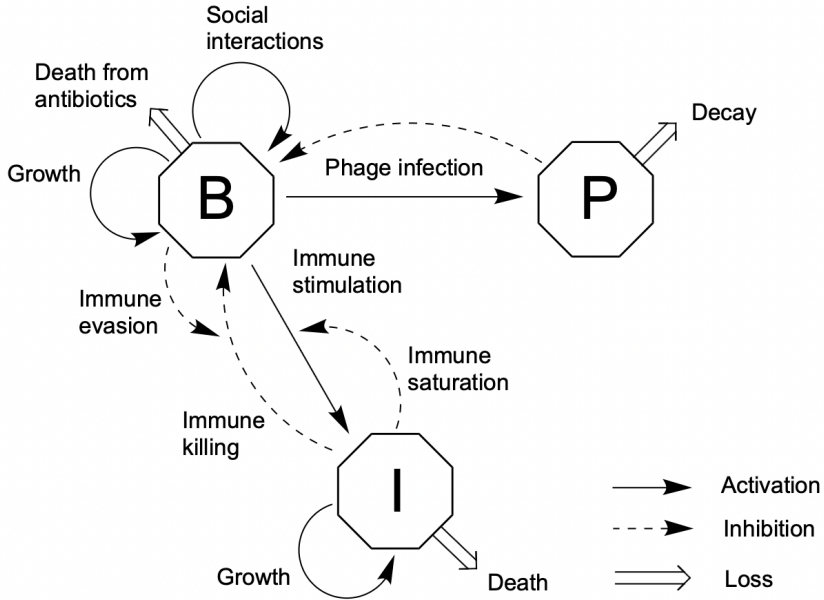


Figure 1: Diagram of the model.  $B$ ,  $I$ , and  $P$  denote bacteria, immune (effector) cells, and phages, respectively.

We designed a system of differential equations to model the dynamics between bacteria, a host's immune response, phages, and antibiotics, which is depicted graphically in Figure 1. Bacteria are killed by immune system effector cells, phages, and antibiotics. However, they also undergo various social interactions among themselves that inhibit the immune response and phage predation (as detailed below). Effector cells are produced at a baseline rate by the host, but bacteria stimulate an immune response thereby increasing their production (Shepherd and McLaren, 2020). Effector cells also die both naturally and by bacterial defenses such as toxins. Phages act as predators to bacterial prey in a Lotka-Volterra model, growing by killing bacteria as well as decaying. The variables  $B$ ,  $I$ , and  $P$  represent the concentrations (in millions per mL) of bacterial cells, immune (ef-

factor) cells, and phages, respectively, and the variable  $A$  represents the concentration of antibiotics in units of mg per L.

The equations for the mathematical model were derived using considerations from previous models of immune system and pathogen dynamics in the literature Barber et al. (2021); Kuznetsov et al. (1994); Leung and Weitz (2017); Reynolds et al. (2006); Shepherd and McLaren (2020). However, previous models of the dynamics of bacteria, the immune system, and phages assume immune saturation similar to a logistic equation (Leung and Weitz, 2017; Rodriguez-Gonzalez et al., 2020). Furthermore, previous models have considered saturating phage adsorption rates using a Hill function of the phage density (Gómez, 2025; Rodriguez-Gonzalez et al., 2020), which models the scenario where multiple phages may bind to the same bacterium thus reducing the effective infection rate. Here, we also assume a Hill function, but of bacterial density, which models the effects of protective social dynamics. Specifically, bacteria have been shown to reduce the number of receptors on their surfaces (phage entry points) in response to quorum sensing signals, halving the phage adsorption rate (Høyland-Kroghsbo et al., 2017). Thus, we assume that the effective adsorption rate is  $\phi/(1 + B/\gamma)$  for parameters  $\phi > 0$  and  $\gamma > 0$ .

The full set of equations for the mathematical model are:

$$\dot{B} = \underbrace{\rho B \left(1 - \frac{B}{\kappa}\right)}_{\text{growth}} - \underbrace{\frac{\epsilon BI}{1 + B/\zeta}}_{\text{death by effector}} - \underbrace{\frac{\phi BP}{1 + B/\gamma}}_{\text{death by phage}} - \underbrace{\frac{\alpha BA^\tau}{A^\tau + \xi^\tau}}_{\text{death by antibiotic}}, \quad (1a)$$

$$\dot{I} = I \left( \underbrace{\frac{\theta B}{B + \eta}}_{\text{activation}} - \underbrace{(\mu B + \delta)}_{\text{death}} \right) + \underbrace{\sigma}_{\text{inflow}}, \quad (1b)$$

$$\dot{P} = \underbrace{\frac{\beta \phi BP}{1 + B/\gamma}}_{\text{replication}} - \underbrace{\omega P}_{\text{decay}}, \quad (1c)$$

$$\dot{A} = \underbrace{D(t)}_{\text{dosing}} - \underbrace{\nu A}_{\text{decay}}. \quad (1d)$$

In Equation 1a, the first term represents the growth rate of bacteria, which is modeled using a logistic growth function with a maximal growth rate of  $\rho$  and carrying capacity  $\kappa$ . The remaining terms of this equation represent the rate bacteria are killed by effector cells and phages, which are reduced by large bacterial populations, and antibiotics. Equation 1b represents the net growth rate of the effector cells. The first term represents the activation of the immune response, the second term represents effector cell death, and the third term is the inflow of new effector cells produced by the host into the region. Finally, Equations 1c and 1d represent the net growth rate of phages as well as the dosing and decay of antibiotics, respectively. Antibiotics are assumed to be administered at regular intervals and are explored numerically in Section 3.2.2. A summary of the parameters and their baseline values can be found in Table 1.

The baseline parameter values for  $\beta$ ,  $\epsilon$ ,  $\zeta$ ,  $\eta$ ,  $\theta$ ,  $\kappa$ ,  $\rho$ ,  $\phi$ , and  $\omega$  are from the parameter values of the model in Leung and Weitz (2017) with data from other studies. Specifically,

Parameter	Definition	Value	Units
$\alpha$	antibiotic kill rate	0.1247	1/hr
$\beta$	phage burst size	100	phages/cell
$\gamma$	quorum sensing threshold	100	$10^6$ cells/mL
$\delta$	effector death rate	0.002	1/hr
$\epsilon$	effector kill rate	0.082	(mL/ $10^6$ )/hr
$\zeta$	immune half saturation	2.2	$10^6$ cells/mL
$\eta$	activation parameter	0.1	$10^6$ cells/mL
$\theta$	maximum activation rate	0.97	1/hr
$\kappa$	carrying capacity of bacteria	1000	$10^6$ cells/mL
$\mu$	inactivation rate	0.01	(mL/ $10^6$ cells)/hr
$\nu$	antibiotic decay rate	0.34657	1/hr
$\xi$	antibiotic half saturation	18.24	mg/L
$\rho$	bacteria growth rate	1	1/hr
$\sigma$	effector birth rate	0.005	$10^6$ cells/hr
$\tau$	Hill coefficient	1.416	—
$\phi$	phage adsorption rate	0.05	1/hr
$\omega$	phage death rate	1	1/hr

Table 1: Summary definitions of parameters and variables.

$\epsilon$  and  $\zeta$  were adapted from Drusano et al. (2011),  $\eta$  was obtained from Sadek et al. (1998) and Wigginton and Kirschner (2001),  $\kappa$  was obtained from Guo et al. (2011),  $\rho$  was obtained from Guo et al. (2011),  $\phi$  was obtained from Shao and Wang (2008) and De Paepe and Taddei (2006), and  $\omega$  was obtained from Hodyra-Stefaniak et al. (2015).  $\theta$  is taken from the maximum growth rate of the immune response calculated in Leung and Weitz (2017) using interstitial neutrophil recruitment data from Reutershan et al. (2005). The immune system model of Leung and Weitz (2017) is similar to ours in that there is a Hill function for activation/stimulation of the immune system. However, their equation includes a density-dependent factor to model immune saturation, and it does not include innate or bacterial induced death rates, nor inflow of immune cells.

The remaining parameter values for the bacteria-immune system-phage system were determined as follows. The birth rate of effector cells  $\sigma$  and the inactivation rate  $\mu$  were taken from Reynolds et al. (2006). The effector death rate  $\delta$  was also taken from Reynolds et al. (2006), sourced from Janeway et al. (2001) and Zouali (2001). It is important to note that the immune system is modeled phenomenologically in this model instead of being cell-specific. Quorum sensing activation is typically observed at bacterial cell densities between  $10^7$  and  $10^9$  cells/mL (Xayarath and Freitag, 2016). We assume it occurs on the order of  $10^8$  bacteria/mL for our baseline scenario, although we explore both an order of magnitude lower and higher in our simulations. Since the effective adsorption rate halved at this value,  $\gamma = 100$ .

Finally, the antibiotic kill rate, half saturation rate, and Hill coefficient for the antibiotic cefoxitin were obtained from Ferro et al. (2015). Cefoxitin was chosen as the antibiotic to be modeled in the simulations due to it being fairly commonly used in clinical settings as well

as the fact that there are many bacteria that are resistant to it (Sartelli et al., 2023; Tebano et al., 2024). The antibiotic decay rate  $\nu$  comes from Brouwers et al. (2020). Antibiotics are assumed to be administered in doses of 100 mg/L, and the initial dose is given at 100 hours. This dosage delay was selected because a study reviewing the median time from bacterial infection to antibiotic treatment found that on average antibiotic treatment is administered approximately 100 hours after initial exposure to the bacterial infection (Holty et al., 2006). After this initial dose, recurring doses are administered on a schedule every 24 hours to simulate an antibiotic that is taken once a day. Similarly, we also assume that phages are introduced as a treatment at 100 hours, though only once as they replicate thereafter.

## 3 Results

### 3.1 Equilibria and stability analysis

Here, we analyze the system without the presence of antibiotics. Equilibria occur when:

$$0 = B \left( \rho \left( 1 - \frac{B}{\kappa} \right) - \frac{\epsilon I}{1 + B/\zeta} - \frac{\phi P}{1 + B/\gamma} \right), \quad (2a)$$

$$0 = I \left( \frac{\theta B}{B + \eta} - \mu B - \delta \right) + \sigma, \quad (2b)$$

$$0 = P \left( \frac{\beta \phi B}{1 + B/\gamma} - \omega \right). \quad (2c)$$

We begin by discussing the bacteria-free and phage-free equilibrium  $\mathcal{E}_1 = (\bar{B}_1, \bar{I}_1, \bar{P}_1) = (0, \sigma/\delta, 0)$ . Following this we will discuss the phage-free bacterial infection equilibria ( $\mathcal{E}_2 = (\bar{B}_2, \bar{I}_2, 0)$ ), and the coexistence of bacteria, effectors, and phages ( $\mathcal{E}_3 = (\bar{B}_3, \bar{I}_3, \bar{P}_3)$ ).  $\mathcal{E}_1$  and  $\mathcal{E}_3$ , if they exist, are unique, while there may be one or three equilibria that satisfy  $\mathcal{E}_2$ . We label these equilibria  $\mathcal{E}_{2a}$ ,  $\mathcal{E}_{2b}$ , and  $\mathcal{E}_{2c}$ . We also note that the Jacobian matrix is:

$$J = \begin{bmatrix} \rho \left( 1 - \frac{2B}{\kappa} \right) - \frac{\epsilon I}{(1 + B/\zeta)^2} - \frac{\phi P}{(1 + B/\gamma)^2} & -\frac{\epsilon B}{1 + B/\zeta} & -\frac{\phi B}{1 + B/\gamma} \\ \left( \frac{\theta \eta}{(B + \eta)^2} - \mu \right) I & \frac{\theta B}{B + \eta} - \mu B - \delta & 0 \\ \frac{\beta \phi P}{(1 + B/\gamma)^2} & 0 & \frac{\beta \phi B}{1 + B/\gamma} - \omega \end{bmatrix}. \quad (3)$$

Evaluating the Jacobian at  $\mathcal{E}_1$  gives us:

$$J(\mathcal{E}_1) = \begin{bmatrix} \rho - \epsilon \bar{I}_1 & 0 & 0 \\ \left( \frac{\theta}{\eta} - \mu \right) \bar{I}_1 & -\delta & 0 \\ 0 & 0 & -\omega \end{bmatrix}. \quad (4)$$

The characteristic equation for this matrix is:

$$(\lambda - \rho + \epsilon \bar{I}_1)(\lambda + \delta)(\lambda + \omega) = 0. \quad (5)$$

This has two negative eigenvalues ( $\lambda_2 = -\delta, \lambda_3 = -\omega$ ) and the last is positive if  $\rho > \epsilon \bar{I}_1$ . Therefore, since we are concerned with the case where bacteria are able to colonize the body, we will assume this inequality holds true for the remainder of the analysis.

$\bar{B}_2^4$ term	$\bar{B}_2^3$ term	$\bar{B}_2^2$ term	$\bar{B}_2$ term	constant term	sign changes
+	+	+	+	-	1
+	+	+	-	-	1
+	+	-	+	-	3
+	+	-	-	-	1
+	-	+	+	-	3
+	-	+	-	-	3
+	-	-	+	-	3
+	-	-	-	-	1

Table 2: Sign and sign changes of the coefficients of Equation 6.

Next, consider  $\mathcal{E}_2 = (\bar{B}_2, \bar{I}_2, 0)$ . Solving  $\dot{B} = 0$ , we have  $\bar{I}_2 = \rho(1 - \bar{B}_2/\kappa)(1 + \bar{B}_2/\zeta)/\epsilon$ . Plugging this into  $\dot{I} = 0$  and simplifying, we get:

$$\begin{aligned} \frac{\mu}{\zeta\kappa} \bar{B}_2^4 + \left( \frac{\eta\mu + \delta - \theta}{\zeta\kappa} + \frac{\mu}{\kappa} - \frac{\mu}{\zeta} \right) \bar{B}_2^3 + \left( \frac{\delta\eta}{\zeta\kappa} + (\theta - \eta\mu - \delta) \left( \frac{1}{\zeta} - \frac{1}{\kappa} \right) - \mu \right) \bar{B}_2^2 \\ + \left( \theta - \eta\mu - \delta - \delta\eta \left( \frac{1}{\zeta} - \frac{1}{\kappa} \right) + \frac{\epsilon\sigma}{\rho} \right) \bar{B}_2 + \frac{\delta\eta}{\rho} (\epsilon\bar{I}_1 - \rho) = 0. \end{aligned} \quad (6)$$

Note that the coefficient of the first term in the polynomial is positive and the last is negative assuming  $\rho > \epsilon\bar{I}_1$ . Thus, by Descartes' Rule of Signs, there are either one or three positive real roots as shown in Table 2. Many of the signs of these terms do not have simple and specific biological meaning. Nonetheless, we can make some general observations. For one, the coefficient of  $\bar{B}_2^3$  is negative when activation of the immune system is sufficiently rapid, which occurs for high  $\theta$  and low  $\eta$ . The effects of high immune activation, however, on coefficients for  $\bar{B}_2^2$  and  $\bar{B}_2$  are more complicated, either increasing or decreasing them. Although, for the baseline parameters in Table 1,  $\zeta < \kappa$  and thus high activation increases the coefficient of  $\bar{B}_2$ .

Returning to our stability analysis, the Jacobian evaluated at  $\mathcal{E}_2$  is:

$$J(\mathcal{E}_2) = \begin{bmatrix} \rho \left( 1 - \frac{2\bar{B}_2}{\kappa} \right) - \frac{\epsilon\bar{I}_2}{(1 + \bar{B}_2/\zeta)^2} & -\frac{\epsilon\bar{B}_2}{1 + \bar{B}_2/\zeta} & -\frac{\phi\bar{B}_2}{1 + \bar{B}_2/\gamma} \\ \left( \frac{\theta\eta}{(\bar{B}_2 + \eta)^2} - \mu \right) \bar{I}_2 & -\frac{\sigma}{\bar{I}_2} & 0 \\ 0 & 0 & \frac{\beta\phi\bar{B}_2}{1 + \bar{B}_2/\gamma} - \omega \end{bmatrix}. \quad (7)$$

And the characteristic equation is:

$$\left(\lambda - \frac{\beta\phi\bar{B}_2}{1+\bar{B}_2/\gamma} + \omega\right) \left(\left(\lambda - \rho\left(1 - \frac{2\bar{B}_2}{\kappa}\right) + \frac{\epsilon\bar{I}_2}{(1+\bar{B}_2/\zeta)^2}\right) \left(\lambda + \frac{\sigma}{\bar{I}_2}\right) + \left(\frac{\theta\eta}{(\bar{B}_2+\eta)^2} - \mu\right) \frac{\epsilon\bar{B}_2\bar{I}_2}{1+\bar{B}_2/\zeta}\right) = 0. \quad (8)$$

From this we can see that  $\bar{B}_2 > 1/(\beta\phi/\omega - 1/\gamma)$  is a sufficient condition for instability of  $\mathcal{E}_2$ . We numerically explore the eigenvalues further in the next section.

Now, consider the case where there is coexistence of all three types ( $\mathcal{E}_3 = (\bar{B}_3, \bar{I}_3, \bar{P}_3)$ ). Solving for  $\dot{P} = 0$  gives us  $\bar{B}_3 = 1/(\beta\phi/\omega - 1/\gamma)$ . Then, we have:

$$\bar{I}_3 = \frac{\sigma}{\mu\bar{B}_3 + \delta - \theta\bar{B}_3/(\bar{B}_3 + \eta)}, \quad (9a)$$

$$\bar{P}_3 = \frac{1 + \bar{B}_3/\gamma}{\phi} \left( \rho \left(1 - \frac{\bar{B}_3}{\kappa}\right) - \frac{\epsilon\bar{I}_3}{1 + \bar{B}_3/\zeta} \right), \quad (9b)$$

assuming that these are positive.

The Jacobian at this equilibrium is:

$$J(\mathcal{E}_3) = \begin{bmatrix} \rho \left(1 - \frac{2\bar{B}_3}{\kappa}\right) - \frac{\epsilon\bar{I}_3}{(1+\bar{B}_3/\zeta)^2} - \frac{\phi\bar{P}_3}{(1+\bar{B}_3/\gamma)^2} & -\frac{\epsilon\bar{B}_3}{1+\bar{B}_3/\zeta} & -\frac{\phi\bar{B}_3}{1+\bar{B}_3/\gamma} \\ \left(\frac{\theta\eta}{(\bar{B}_3+\eta)^2} - \mu\right)\bar{I}_3 & -\frac{\sigma}{\bar{I}_3} & 0 \\ \frac{\beta\phi\bar{P}_3}{(1+\bar{B}_3/\gamma)^2} & 0 & 0 \end{bmatrix}, \quad (10)$$

and it has the characteristic equation:

$$\left(\lambda + \frac{\sigma}{\bar{I}_3}\right) \left(\lambda^2 + \left(\frac{\epsilon\bar{I}_3}{(1+\bar{B}_3/\zeta)^2} + \frac{\phi\bar{P}_3}{(1+\bar{B}_3/\gamma)^2} - \rho \left(1 - \frac{2\bar{B}_3}{\kappa}\right)\right) \lambda + \frac{\beta\phi^2\bar{B}_3\bar{P}_3}{(1+\bar{B}_3/\gamma)^3}\right) = 0. \quad (11)$$

Note that  $\lambda_1 = -\sigma/\bar{I}_3 < 0$  and:

$$\frac{\epsilon\bar{I}_3}{(1+\bar{B}_3/\zeta)^2} + \frac{\phi\bar{P}_3}{(1+\bar{B}_3/\gamma)^2} - \rho \left(1 - \frac{2\bar{B}_3}{\kappa}\right) = \bar{B}_3 \left(-\frac{\epsilon\bar{I}_3/\zeta}{(1+\bar{B}_3/\zeta)^2} - \frac{\phi\bar{P}_3/\gamma}{(1+\bar{B}_3/\gamma)^2} + \frac{\rho}{\kappa}\right). \quad (12)$$

If  $\gamma, \zeta \gg 0$ , then all the coefficients of the quadratic in Equation 11 are positive, and thus the equilibrium is stable. Otherwise, it may not be. We explore the eigenvalues numerically in the next section.

## 3.2 Numerical results

### 3.2.1 Bifurcation diagrams

We begin with an exploration of parameter space by individually varying the parameters from Table 1 before considering specific scenarios. Figure 2 depicts these bifurcation diagrams. Red corresponds to unstable equilibria and blue to stable equilibria. This results in either a low bacterial population density or even no bacteria altogether. It is important to

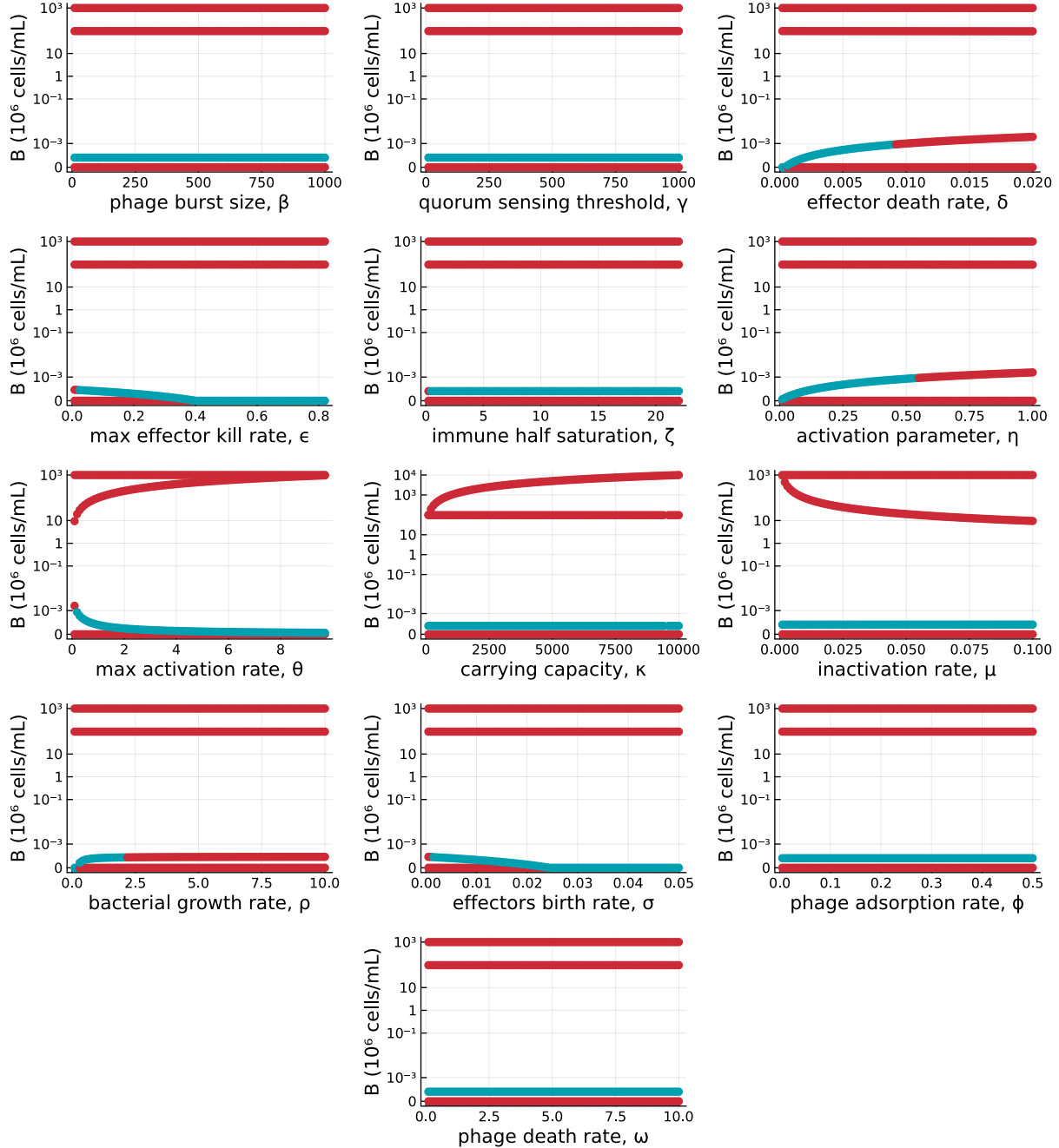


Figure 2: Bifurcation diagrams for equilibrium number of bacteria  $\bar{B}_i$ . Parameters are varied from one tenth to ten times the baseline values in Table 1. Blue indicates a stable equilibrium and red a saddle. The vertical axis is plotted in symmetrical log scale: data is converted via the function  $\text{symlog}(x) = \log_{10}(1 + 10^3 x)$ .

note that the y-axes of these plots correspond with the bacterial density measured in millions of cells per mL. For example, a bacterial density of  $10^{-3}$  indicates a bacterial density of  $10^3$  cells per mL.

Across all diagrams, there is either a single stable equilibrium with a relatively low

density of bacteria or no stable equilibria. The latter scenario results in oscillations, which we will discuss in depth in Section 3.2.2. The bifurcation plots for  $\beta$ ,  $\gamma$ ,  $\kappa$ ,  $\mu$ ,  $\phi$ , and  $\omega$  all lack a bifurcation point where the stable equilibrium becomes unstable, showing a robustness of the qualitative results with respect to these parameters. The remaining parameters exhibit bifurcation points. For  $\delta$ , we observe a bifurcation point at  $\delta \approx 0.009$ . Below this point, there is the single stable equilibrium and above it all equilibria are unstable.  $\epsilon$  has a bifurcation point corresponding with low densities of bacteria at  $\epsilon \approx 0.01$ . Likewise, the bifurcation plot of  $\zeta$  shows a bifurcation point at  $\zeta \approx 0.1$ . The bifurcation plot of  $\eta$  indicates a bifurcation point corresponding to a bacterial density of  $10^{-3}$  and  $\eta \approx 0.55$ . At very low values of  $\theta$  and a bacterial density of approximately  $10^{-3}$ , a bifurcation point exists for the parameter  $\theta$ . For the parameter  $\rho$ , there appear to be two bifurcation points. One of these points corresponds with the bacteria free state and very small values of  $\rho$ . This result mirrors our analytical findings: for sufficiently low  $\rho$ , the bacteria-free equilibrium is the sole stable equilibrium. The other bifurcation point occurs at low bacterial densities and when  $\rho \approx 2$ . Finally, the bifurcation diagram generated for  $\sigma$  shows a bifurcation point at low bacterial densities and very small values of  $\sigma$ .

### 3.2.2 Time series

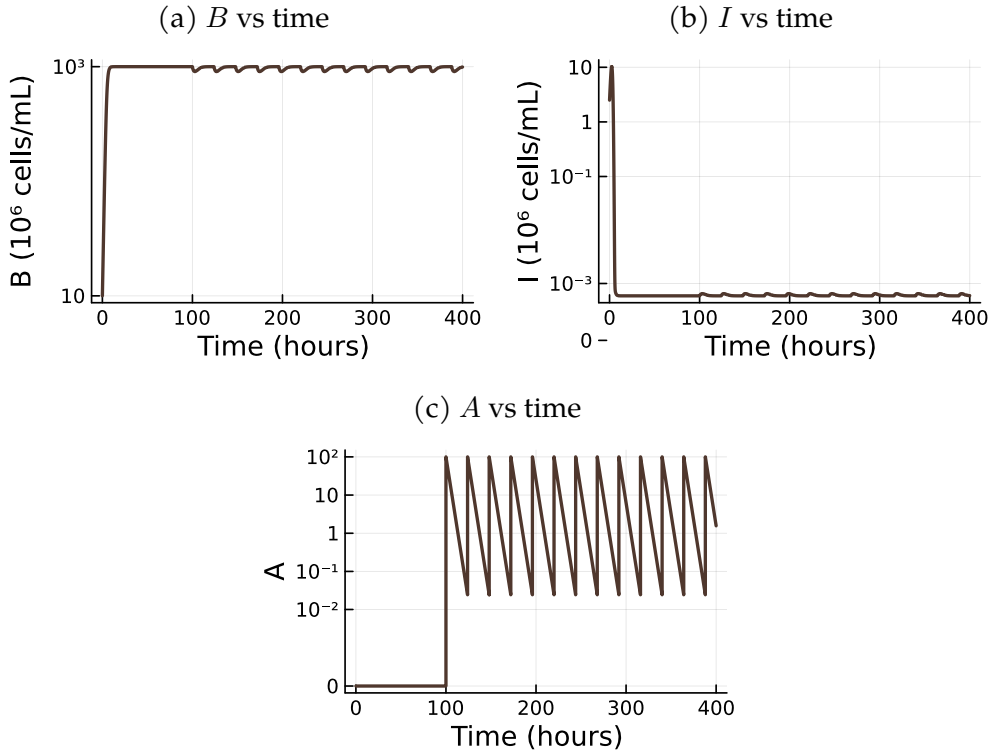


Figure 3: Time series plots for the case with periodic applications of antibiotics, but no phages are present. Parameters are taken from Table 1. Antibiotics alone are unable to control and suppress the infection. The vertical axis is plotted in symmetrical log scale: data is converted via the function  $\text{symlog}(x) = \log_{10}(1 + 10^3 x)$ .

In this section, we begin with a demonstration of the case where no phages are present and only antibiotics are used to attempt to suppress the infection. Figure 3 depicts the time series plots for this case. The initial conditions are  $B_0 = 10$  and  $I_0 = \sigma/\delta$ , which allow for the bacteria to escape immune suppression, approach the carrying capacity, and enervate the immune response. After 100 hours, the antibiotic is applied at regular daily intervals. However, this therapy is insufficient in quelling the infection.

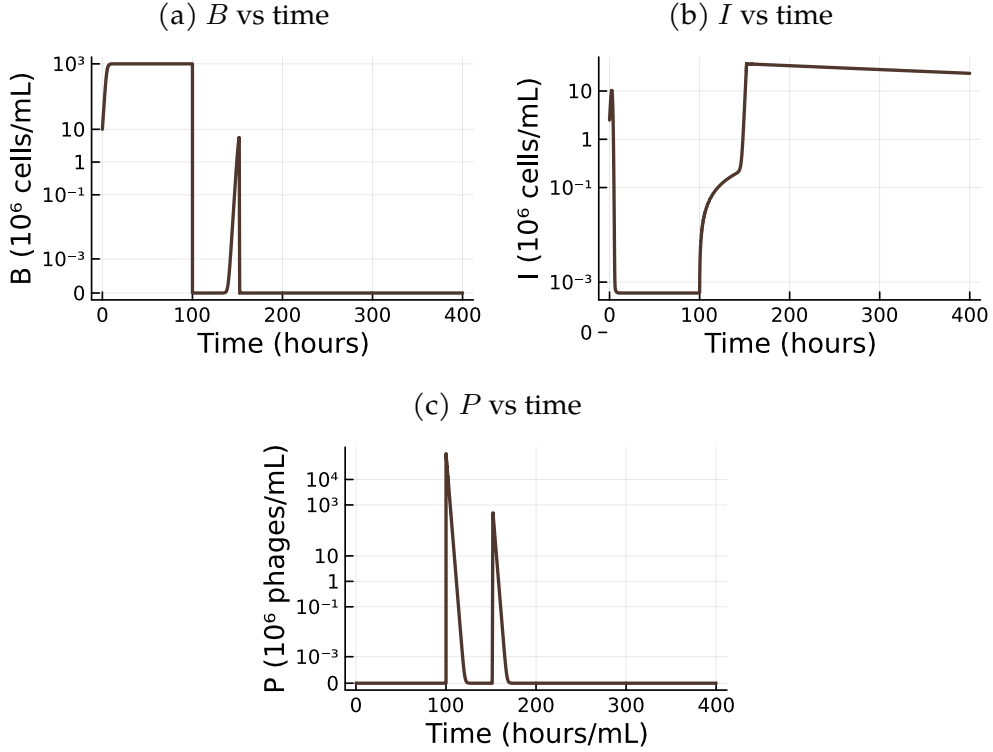


Figure 4: Time series plots for the baseline scenario with parameters from Table 1. Phage therapy successfully assists the immune system in suppressing the infection. The vertical axis is plotted in symmetrical log scale: data is converted via the function  $\text{symlog}(x) = \log_{10}(1 + 10^3 x)$ .

Equilibrium	B	I	P	Eigenvalues
$\mathcal{E}_1$	0	2.5	0	2 negative real and 1 positive real
$\mathcal{E}_{2a}$	0.0001643598	12.19603	0	1 negative real, complex pair with negative real part
$\mathcal{E}_{2b}$	96.70080	495.21628	0	2 positive real, 1 negative real
$\mathcal{E}_{2c}$	999.9999	0.0005535814	0	1 positive real, 2 negative real
$\mathcal{E}_3$	DNE	DNE	DNE	N/A

Table 3: Summary of equilibria found numerically.

Next, consider a phage treatment with the same initial conditions of  $B_0 = 10$  and  $I_0 =$

$\sigma/\delta$  where treatment is initiated after 100 hours. As seen in the time series plots in Figure 4, phage therapy is able to control the infection. Phage density increases rapidly, bacterial density crashes, and effector cell density rebounds. Indeed, with the presence of phages, the system has a sole stable equilibrium with low bacterial density. Table 3 details all of the numerically found equilibria, of which there are four, and the nature of their eigenvalues. The first equilibrium ( $\mathcal{E}_1$ ) is the bacteria and phage free state, which is unstable. Two of the three phage-free equilibria ( $\mathcal{E}_{2b}$  and  $\mathcal{E}_{2c}$ ) are saddle points, and the other equilibrium ( $\mathcal{E}_{2a}$ ) is stable. Phages are unable to persist with bacteria at this density. Nonetheless, phages are crucial in undermining the stability of the high bacterial density equilibrium ( $\mathcal{E}_{2c}$ ). The last potential equilibrium point, corresponding to the coexistence of bacteria, effectors, and phages, does not exist for these parameter values ( $\bar{I}_3$  is negative). Although bacteria do still persist at low levels in this scenario, there are practical considerations that suggest they would be eliminated. In examining the time series plots, the minimum bacterial density reaches approximately  $10^{-18}$  cells/mL after the introduction of phages. Though it oscillates as it equilibrates to approximately 164 bacteria per mL, the bacteria would in effect be eliminated earlier.

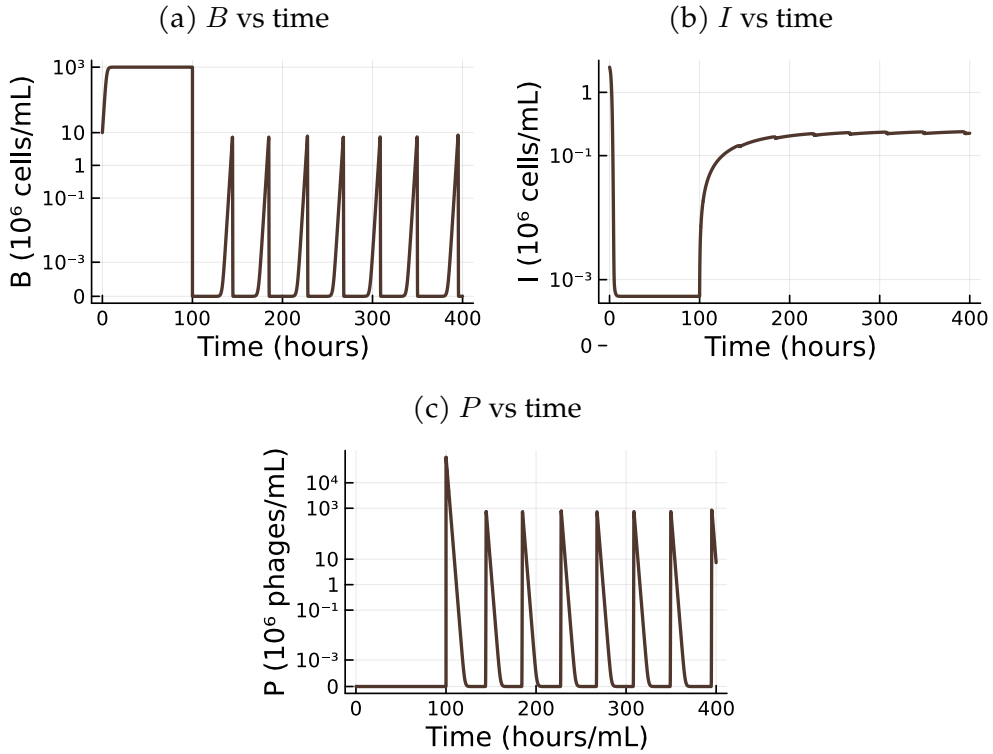


Figure 5: Time series plots for the immunodeficient host scenario.  $\delta = 0.02$ ,  $\eta = 1.0$ , and  $\theta = 0.01$  while remaining parameters are taken from Table 1. The system is oscillatory. The vertical axis is plotted in symmetrical log scale: data is converted via the function  $\text{symlog}(x) = \log_{10}(1 + 10^3x)$ .

The results above reflect the scenarios from the bifurcation diagrams with only a single stable equilibrium at relatively low bacterial densities. We now consider time series for

the second regime where there are no stable equilibria (using the same initial conditions and timing of treatment). Note that a few of these correspond to immunodeficient hosts: effector activation is low, which can occur via low  $\theta$  or high  $\eta$ , or effector death rates are high. High bacterial growth rates can also result in no stable equilibria. Under these scenarios, the population density oscillates. Figure 5a depicts this scenario with  $\delta = 0.02$ ,  $\eta = 1.0$ , and  $\theta = 0.01$ . These oscillations bring bacterial density to elimination levels (approximately  $10^{-13}$  bacteria per mL). A theoretical novelty of the system is that the results suggest chaotic behaviour. We numerically calculated the Lyapunov exponent, finding that it was positive, indicating chaos. However, as stated above, population levels reach extremely low values and thus the bacteria are effectively eliminated. A combination therapy of phages and antibiotics can drive bacterial densities even lower (the results for this case and apparent chaos are not shown here, although they are reproducible via the code).

Interestingly, these large oscillations are in large part due to quorum sensing mediated bacterial protections from phages. For comparison, consider the model of Leung and Weitz (2017), which features a Holling type I functional response. It exhibits instability of oscillations when there are only bacteria and phages interacting. However, this occurs on long time scales. The Holling type II functional response that we consider accelerates this instability. By weakening phage predation, bacteria can grow to higher densities before being subdued by phages, which in turn results in large phage populations. Bacteria then lose their defenses as their density drops below the quorum sensing threshold, exacerbating their decline. The short term benefits of phage protection ultimately dooms the bacteria to elimination. Furthermore, there is a game theory insight into this result. In a heterogeneous population of bacteria, there is an incentive for individual bacterial clusters to quorum sense for their own immediate protection, even though abstaining would benefit the population as a whole. In a sense, bacteria that reduce their receptors due to quorum-sensing are free-riders or defectors, while those that do not are cooperators.

## 4 Discussion

The dynamics behind phage therapy in clinical settings are not fully understood, since the exact interactions between bacteria, immune cells, and phages are oftentimes very complex. To better understand these dynamics, we developed a model that incorporates the social behaviors of bacteria, an innate immune response, phages, and periodic antibiotic dosing. This model is similar to Leung and Weitz (2017), though with different assumptions regarding the immune response. We assume a constant inflow of effector cells into the infected region along with bacteria-mediated death of effector cells. Structurally, our model, not including the phages, is similar to the immuno-tumor model of Kuznetsov et al. (1994), which has also been extended to explore social dynamics (Morsky and Vural, 2018).

Our results indicate that the system has a single stable equilibrium for our baseline parameters in which effectors and low levels of bacteria coexist. Phage therapy has effectively eliminated the stable equilibrium with a large population of bacteria, and the immune system is thus able to contain the bacterial infection. Even for immunodeficient

hosts, phage therapy results in such large oscillations in the population of bacteria that they would effectively be eliminated. This effect is further aided by the assistance of antibiotics in a combination therapy. This result has similarity to the finding from Leung and Weitz (2017) where it was observed that phage therapy and the host's immune system were able to eradicate the bacterial infection in the normal mice population but not in the neutropenic mice population. However, the presence of quorum-sensing mediated bacterial defenses in our model essentially results in elimination of the infection even in immunodeficient hosts.

The proposed model allows for analytical and numerical solutions to be found for the conditions where phages and the immune response can kill bacteria. However, this synergistic effect is a simplification made to be able to analyze a much more complex dynamic. One assumption that was made is that there is only one type of bacteria in the system that has a consistent reaction to the phages and immune response. In reality, the interactions between bacteria, an immune system, and phages are much more complex. In particular, bacteria are able to develop phage resistance by modifying the cell surface receptors that phages attach onto (Labrie et al., 2010). However, it has been noted that increased phage resistance oftentimes leads to increased susceptibility to antibiotics (Chan et al., 2016). As a result, a future study could explore an expansion of the model presented here with multiple bacterial species, mutations, and trade-offs for resistance to phages and antibiotics. Combination therapies that leverage these trade-offs — such as switching environmental regimes (Morsky and Vural, 2022) — could be explored to determine optimal treatments to control the bacteria. Finally, it has been demonstrated that both the innate and adaptive immune responses can actively eliminate phages (Hodyra-Stefaniak et al., 2015). This process can and would likely impact the overall effectiveness of phage therapy in a clinical context. In our model, the death rate of phages is assumed to be constant, represented by the parameter  $\omega$ , and determined by the density of bacteria. However, phages could also be killed by the immune system and help activate it. In this case, the effectiveness of phage therapy could be tied to the relationship between the killing of phages by the immune system and their synergistic elimination of bacteria.

## Code and Data Availability

Numerical methods in Julia were used to identify equilibria and characterize their stability. Specifically, the DifferentialEquations.jl package (Rackauckas and Nie, 2017) was employed to numerically solve the system. The code to solve the equations numerically and produce the plots is available at [github.com/bmorsky/phage-therapy](https://github.com/bmorsky/phage-therapy).

## References

Abisado, R. G., Benomar, S., Klaus, J. R., Dandekar, A. A., and Chandler, J. R. (2018). Bacterial quorum sensing and microbial community interactions. *MBio*, 9(3):10–1128.

Akkaya, M., Kwak, K., and Pierce, S. K. (2020). B cell memory: building two walls of protection against pathogens. *Nature Reviews Immunology*, 20(4):229–238.

Barber, J., Carpenter, A., Torsey, A., Borgard, T., Namas, R. A., Vodovotz, Y., and Arciero, J. (2021). Predicting experimental sepsis survival with a mathematical model of acute inflammation. *Frontiers in Systems Biology*, 1:755913.

Barbosa, T. M. and Levy, S. B. (2000). The impact of antibiotic use on resistance development and persistence. *Drug resistance updates*, 3(5):303–311.

Blanden, R. (1974). T cell response to viral and bacterial infection. *Immunological Reviews*, 19(1):56–88.

Brouwers, R., Vass, H., Dawson, A., Squires, T., Tavaddod, S., and Allen, R. J. (2020). Stability of  $\beta$ -lactam antibiotics in bacterial growth media. *PLoS one*, 15(7):e0236198.

Burmeister, A. R. (2015). Horizontal gene transfer. *Evolution, medicine, and public health*, 2015(1):193–194.

Chan, B. K., Sistrom, M., Wertz, J. E., Kortright, K. E., Narayan, D., and Turner, P. E. (2016). Phage selection restores antibiotic sensitivity in mdr *pseudomonas aeruginosa*. *Scientific reports*, 6(1):26717.

De Paepe, M. and Taddei, F. (2006). Viruses' life history: towards a mechanistic basis of a trade-off between survival and reproduction among phages. *PLoS biology*, 4(7):e193.

Drusano, G., Vanscoy, B., Liu, W., Fikes, S., Brown, D., and Louie, A. (2011). Saturability of granulocyte kill of *pseudomonas aeruginosa* in a murine model of pneumonia. *Antimicrobial agents and chemotherapy*, 55(6):2693–2695.

Eriksen, R. S., Svenningsen, S. L., Sneppen, K., and Mitarai, N. (2018). A growing microcolony can survive and support persistent propagation of virulent phages. *Proceedings of the National Academy of Sciences*, 115(2):337–342.

Ferro, B. E., van Ingen, J., Wattenberg, M., van Soolingen, D., and Mouton, J. W. (2015). Time-kill kinetics of antibiotics active against rapidly growing mycobacteria. *Journal of Antimicrobial Chemotherapy*, 70(3):811–817.

Flores-Garza, E., Zetter, M. A., Hernández-Pando, R., and Domínguez-Hüttinger, E. (2022). Mathematical model of the immunopathological progression of tuberculosis. *Frontiers in Systems Biology*, 2:912974.

Fujiki, J. and Schnabl, B. (2023). Phage therapy: targeting intestinal bacterial microbiota for the treatment of liver diseases. *Jhep Reports*, 5(12):100909.

Gestel, J. V., Vlamakis, H., and Kolter, R. (2015). Division of labor in biofilms: the ecology of cell differentiation. *Microbial Biofilms*, pages 67–97.

Giamarellos-Bourboulis, E. J. and Raftogiannis, M. (2012). The immune response to severe bacterial infections: consequences for therapy. *Expert review of anti-infective therapy*, 10(3):369–380.

Gómez, M. C. (2025). Mathematical model of the interaction of pathogenic bacteria and bacteriophages. *Proceeding Series of the Brazilian Society of Computational and Applied Mathematics*, 11(1):1–5.

Gordillo Altamirano, F. L. and Barr, J. J. (2019). Phage therapy in the postantibiotic era. *Clinical microbiology reviews*, 32(2):10–1128.

Guo, B., Abdelraouf, K., Ledesma, K. R., Chang, K.-T., Nikolaou, M., and Tam, V. H. (2011). Quantitative impact of neutrophils on bacterial clearance in a murine pneumonia model. *Antimicrobial agents and chemotherapy*, 55(10):4601–4605.

Hansen, M. F., Svenningsen, S. L., Røder, H. L., Middelboe, M., and Burmølle, M. (2019). Big impact of the tiny: bacteriophage–bacteria interactions in biofilms. *Trends in microbiology*, 27(9):739–752.

Harrison, F., Browning, L. E., Vos, M., and Buckling, A. (2006). Cooperation and virulence in acute *pseudomonas aeruginosa* infections. *BMC biology*, 4(1):21.

Hodyra-Stefaniak, K., Miernikiewicz, P., Drapała, J., Drab, M., Jończyk-Matysiak, E., Lecion, D., Kaźmierczak, Z., Beta, W., Majewska, J., Harhala, M., et al. (2015). Mammalian host-versus-phage immune response determines phage fate in vivo. *Scientific reports*, 5(1):14802.

Holty, J.-E. C., Bravata, D. M., Liu, H., Olshen, R. A., McDonald, K. M., and Owens, D. K. (2006). Systematic review: a century of inhalational anthrax cases from 1900 to 2005. *Annals of internal medicine*, 144(4):270–280.

Høyland-Kroghsbo, N. M., Paczkowski, J., Mukherjee, S., Broniewski, J., Westra, E., Bondy-Denomy, J., and Bassler, B. L. (2017). Quorum sensing controls the *pseudomonas aeruginosa* crispr-cas adaptive immune system. *Proceedings of the National Academy of Sciences*, 114(1):131–135.

Ibberson, C. B. and Whiteley, M. (2020). The social life of microbes in chronic infection. *Current opinion in microbiology*, 53:44–50.

Janeway, C. A. J., Travers, P., Walport, M., and Shlomchik, M. J. (2001). *Immunobiology: The Immune System in Health and Disease*. Garland Science, New York, 5th edition.

Jarrett, A. M., Cogan, N., and Shirtliff, M. (2015). Modelling the interaction between the host immune response, bacterial dynamics and inflammatory damage in comparison with immunomodulation and vaccination experiments. *Mathematical medicine and biology: a journal of the IMA*, 32(3):285–306.

Javaudin, F., Latour, C., Debarbieux, L., and Lamy-Besnier, Q. (2021). Intestinal bacteriophage therapy: looking for optimal efficacy. *Clinical Microbiology Reviews*, 34(4):e00136–21.

Jefferson, K. K. (2004). What drives bacteria to produce a biofilm? *FEMS microbiology letters*, 236(2):163–173.

Kostakioti, M., Hadjifrangiskou, M., and Hultgren, S. J. (2013). Bacterial biofilms: development, dispersal, and therapeutic strategies in the dawn of the postantibiotic era. *Cold Spring Harbor perspectives in medicine*, 3(4):a010306.

Kuznetsov, V. A., Makalkin, I. A., Taylor, M. A., and Perelson, A. S. (1994). Nonlinear dynamics of immunogenic tumors: parameter estimation and global bifurcation analysis. *Bulletin of mathematical biology*, 56(2):295–321.

Labrie, S. J., Samson, J. E., and Moineau, S. (2010). Bacteriophage resistance mechanisms. *Nature Reviews Microbiology*, 8(5):317–327.

Leung, C. Y. J. and Weitz, J. S. (2017). Modeling the synergistic elimination of bacteria by phage and the innate immune system. *Journal of Theoretical Biology*, 429:241–252.

Levin, B. R. and Bull, J. J. (2004). Population and evolutionary dynamics of phage therapy. *Nature Reviews Microbiology*, 2(2):166–173.

Morsky, B. and Vural, D. C. (2018). Cheater-altruist synergy in public goods games. *Journal of Theoretical Biology*, 454:231–239.

Morsky, B. and Vural, D. C. (2022). Suppressing evolution of antibiotic resistance through environmental switching. *Theoretical Ecology*, 15(2):115–127.

Normark, B. H. and Normark, S. (2002). Evolution and spread of antibiotic resistance. *Journal of internal medicine*, 252(2):91–106.

Rackauckas, C. and Nie, Q. (2017). DifferentialEquations.jl—a performant and feature-rich ecosystem for solving differential equations in Julia. *Journal of Open Research Software*, 5(1).

Reutershan, J., Basit, A., Galkina, E. V., and Ley, K. (2005). Sequential recruitment of neutrophils into lung and bronchoalveolar lavage fluid in lps-induced acute lung injury. *American Journal of Physiology-Lung Cellular and Molecular Physiology*, 289(5):L807–L815.

Reynolds, A., Rubin, J., Clermont, G., Day, J., Vodovotz, Y., and Ermentrout, G. B. (2006). A reduced mathematical model of the acute inflammatory response: I. derivation of model and analysis of anti-inflammation. *Journal of theoretical biology*, 242(1):220–236.

Rodriguez-Gonzalez, R. A., Leung, C. Y., Chan, B. K., Turner, P. E., and Weitz, J. S. (2020). Quantitative models of phage-antibiotic combination therapy. *mSystems*, 5(1):e00756–19.

Ross-Gillespie, A., Gardner, A., Buckling, A., West, S. A., and Griffin, A. S. (2009). Density dependence and cooperation: theory and a test with bacteria. *Evolution*, 63(9):2315–2325.

Sadek, M. I., Sada, E., Toossi, Z., Schwander, S. K., and Rich, E. A. (1998). Chemokines induced by infection of mononuclear phagocytes with mycobacteria and present in lung alveoli during active pulmonary tuberculosis. *American journal of respiratory cell and molecular biology*, 19(3):513–521.

Sartelli, M., Boermeester, M. A., Cainzos, M., Cocolini, F., de Jonge, S. W., Rasa, K., Dellinger, E. P., McNamara, D. A., Fry, D. E., Cui, Y., et al. (2023). Six long-standing questions about antibiotic prophylaxis in surgery. *Antibiotics*, 12(5):908.

Shao, Y. and Wang, I.-N. (2008). Bacteriophage adsorption rate and optimal lysis time. *Genetics*, 180(1):471–482.

Shepherd, F. R. and McLaren, J. E. (2020). T cell immunity to bacterial pathogens: mechanisms of immune control and bacterial evasion. *International journal of molecular sciences*, 21(17):6144.

Simmons, E. L., Bond, M. C., Koskella, B., Drescher, K., Bucci, V., and Nadell, C. D. (2020). Biofilm structure promotes coexistence of phage-resistant and phage-susceptible bacteria. *MSystems*, 5(3):10–1128.

Singh, A., Padmesh, S., Dwivedi, M., and Kostova, I. (2022). How good are bacteriophages as an alternative therapy to mitigate biofilms of nosocomial infections. *Infection and Drug Resistance*, pages 503–532.

Tebano, G., Zaghi, I., Cricca, M., and Cristini, F. (2024). Antibiotic treatment of infections caused by ampc-producing enterobacteriales. *Pharmacy*, 12(5):142.

Uyttebroek, S., Chen, B., Onsea, J., Ruythooren, F., Debaveye, Y., Devolder, D., Spriet, I., Depypere, M., Wagemans, J., Lavigne, R., et al. (2022). Safety and efficacy of phage therapy in difficult-to-treat infections: a systematic review. *The Lancet Infectious Diseases*, 22(8):e208–e220.

West, S. A., Diggle, S. P., Buckling, A., Gardner, A., and Griffin, A. S. (2007). The social lives of microbes. *Annu. Rev. Ecol. Evol. Syst.*, 38(1):53–77.

Wigginton, J. E. and Kirschner, D. (2001). A model to predict cell-mediated immune regulatory mechanisms during human infection with mycobacterium tuberculosis. *The Journal of Immunology*, 166(3):1951–1967.

Xayarath, B. and Freitag, N. E. (2016). When being alone is enough: noncanonical functions of canonical bacterial quorum-sensing systems. *Future Microbiology*, 11(11):1447–1459.

Zalewska, A., Jurczak-Kurek, A., Kwiatek, M., Myung, H., and Górnjak, M. (2025). Insights into the molecular determinants of host specificity in pseudomonas aeruginosa-infecting phages: a structural and functional analysis of tail fibre proteins. *BMC biology*, 23(1):342.

Zhao, J., Quan, C., Jin, L., and Chen, M. (2018). Production, detection and application perspectives of quorum sensing autoinducer-2 in bacteria. *Journal of Biotechnology*, 268:53–60.

Zouali, M. (2001). Antibodies. In *Encyclopedia of Life Science*. Nature Publishing Group.